Delineation of Groundwater Potential Zones in Nuweiba Area (Egypt) Using Remote Sensing and GIS Techniques

Sara M. Abuzied[1, 3], May Yuan[2], Samia K. Ibrahim[3], Mona F. Kaiser[3], and Tarek A. Seleem[3]
[1]Center for Spatial analysis, University of Oklahoma, Norman, USA
[2]Program of Geospatial Information Science, University of Texas at Dallas, Dallas, USA
[3]Geology Department, Suez Canal University, Ismailia, Egypt
Email: saraabozied@ou.edu

Abstract—**The exploration of new locations for possible groundwater discharge is required to support the needs of urban and agricultural activities in arid regions, such as the Nuweiba area. The aim of this study is to locate new groundwater wells in the Nuweiba area to alleviate water shortage. We identified several essential factors contributing to groundwater discharge. These factors include textural classification of alluvial deposits, lithological units, surface and subsurface structures, topographic parameters, geomorphological features and land use land cover. We developed a hydrogeological model incorporating these factors. Input data to the model include SPOT5, SRTM, Radarsat-1, ALOS PALSAR, GPR, and geologic and topographic maps. The model ingested these data as rasters and determines weights to integrate the contributing factors spatially. The groundwater potential map was classified to five classes from very poor to very good potential. The classes of groundwater potential map were checked against the distribution of the groundwater wells in Bedouin communities and agriculture areas, which present a general knowledge of groundwater potential in the study area.**

***Index Terms*—radar, groundwater potential zones, weightage analysis, remote sensing, GIS, nuweiba**

I. Introduction

Assessing water resources and impacts on the environment are essential for the development of Nuweiba area. Remote sensing and GIS tools were widely used for the management of water resources [1], [2]. Several studies supported assessment of groundwater potential zones using satellite data along with conventional maps and rectified ground truth data [3], [4]. Several parameters including lithology, geomorphology, faults, lineaments, land use/land cover, drainage, elevation and slope affect spatial characteristics of groundwater [5]. These parameters were given different weights of importance and different classes in considering individual influences on groundwater occurrence. Several previous studies identified the groundwater potential zones using the integration of different thematic layers in a GIS with fixed score and weight for each layer [6], [7]. Therefore, this study aims to develop a hydrogeological model of groundwater availability in the Nuweiba area using geological, geomorphological and topographical information. The preparation of thematic maps including lithology, lineaments, faults, landforms, elevation and slopes from remotely sensed data and field studies, is the important task for that purpose. The groundwater potential zones were delineated through integration of these weighted thematic maps.

In the current study, different techniques were performed to evaluate groundwater potential zones using different types of data including SAR, GPR, SRTM, SPOT5, geologic, and topographic maps. These data were processed, interpreted, and spatially integrated using popular remote sensing and GIS software packages (ENVI5.0 and ArcMap 10.2). Different sources of radar imagery including Radarsat-1 and ALOS PALSAR were used to define textural characteristics of alluvial deposits and shallow subsurface structure in the Nuweiba area. C-band of Radarsat-1 contributed SAR data for classifying textural characteristics of alluvial deposits [8]. L-bands of ALOS PALSAR and Ground Penetrating Radar (GPR) provided SAR data for detecting the buried fault in the western desert of Egypt [9]. Digital Elevation Models (DEMs) from the Shuttle Radar Topography Mission (SRTM) were used to create various thematic maps including geomorphology, drainage density, and slope maps.

II. Geological Charcteristics of the Study Area

The Nuweiba area is on an alluvial fan, from the main channel of Wadi Watir to the Gulf of Aqaba between latitudes 28°45' and 29°35' N and longitudes 33°53' and 34° 47' E covering approximately 1,600 km^2 (Fig. 1). The study area is characterized with rugged mountainous topography and high relief on the both sides of W. Watir. Its relief varies from gently inclined plains to rugged steep mountains with elevations from 33m to 1581m above sea level. Nuweiba is in an arid to semi-arid climate area in which summers are very hot and dry, and winters are mild with intense rain. It geology is

Manuscript received November 10, 2014; revised March 20, 2015.

doi: 10.12720/ijsps.4.2.109-117

characterized by lithological units and structural elements as described below.

A. Lithological Units

SPOT5 (band 1, 2, 3 and Panchromatic at 5m×5m) were processed in ENVI 5.0 (Exelis, Boulder, Colorado, United States) to identify different rock units using a mixture of unsupervised classification and supervised maximum likelihood classification based on training classes derived from the field investigations and geological maps [10]. The Kappa Coefficient technique [11] was used to evaluate the accuracy of the classification. The rock units were classified essentially based on physical and hydrological characteristics.

Lithologically, the Nuweiba area is part of the Precambrian Arabian-Nubian Massif that extends across southern Sinai to western Saudi Arabia [12]. The Nuweiba area includes two main lithological groups, namely the Precambrian basement rock and Phanerozoic sedimentary succession with different hydrological properties. The Precambrian basement covers 34% of the area; and the Phanerozoic sedimentary succession covers the rest of the area. The Precambrian basement rock includes both metamorphic and igneous rocks which follow the steep hills along the main wadis, and the steep slope expedites runoff accumulation into the wadis. The Phanerozoic sedimentary succession was classified to three divisions: the lower clastic division of lower cretaceous covering 16% of the study area; the middle calcareous of Cenomanian to Eocene covering 24%; and the upper clastic division of the Neogene to Holocene age covering 26%. The upper and lower divisions are high permeable, separated by the low permeable middle division.

B. Structural Elements

Structural elements, including faults, fractures, and joints, have a significant role for the hydrogeological setting in the Nuweiba area. The structural elements act as a major passage for groundwater and form a substantial part of the reservoir in the Nuweiba area. For hydrogeological assessment, the identification of these linear features is significant, since they reflect fracture traces with high infiltration and groundwater potential. Hence, we performed a lineaments analysis to understand the relationship between the lineament trends and zones of high aquifer recharge. The lineaments analysis applied remote sensing and GIS techniques with the existing geological data and field measurements. Several software were used for this purpose including PCI Geomatica, ENVI 5.0, ArcMap 10.2, and Rockworks 1.6.

Lineament extraction was performed in two main steps: manual extraction and automatic extraction. The manual extraction aims to delineate the major faults which can be visually identified on the imagery. Images from two sensors were utilized for that purpose. These sensors include two full scenes of SPOT5 (MS: 10m & Pan: 5m) and four mosaic scenes of ALOS PALSAR (L-band: 4.6×6.2 m). SPOT5 scenes represent the optical data of which the first 4 reflective bands with a spatial resolution of 10m and the panchromatic band 5 with 5m spatial resolution. These scenes were acquired on 17-12-2011. Four scenes of ALOS PALSAR (L-band, HH-polarization, and ascending orbit) scenes with an incidence angle of 35.085 degree. Due to the smaller footprint of the fine resolution PALSAR scenes (70×60 km^2) a total of four scenes were needed to cover the entire Nuweiba area. Four images from ALOS PALSAR/SPOT5 (band 1, 2, 3, Pan. for SPOT5, and L-band for SAR) were fused for lineament extraction (Fig. 2). The following steps were taken to fuse optical and microwave datasets:

- The four SPOT5 bands (1, 2, 3, and SWIR) were sharpened using panchromatic in the Gramm-Schmidt Sharpening method in ENVI 5.0.
- SAR dataset imported, geocoded and calibrated using SARscape module of ENVI 5.0
- SAR dataset geo-referenced to a common UTM coordinate system.
- A Lee-enhanced filter with a kernel size of 5×5 was applied to raw SAR datasets.
- Ground controls points (GCP) were selected for resampling the SAR filtered images to the same pixel size of SPOT5 (5m.) using 30 well distributed points (0.38 RMS error). The GCPs were selected in the flat alluvial areas to avoid topographic distortion correction of SAR which compensate for foreshortening, layover, and shadow effects in mountainous areas. The SAR images were resampled to the same pixel size as the SPOT5 panchromatic (5m) image using 40 well distributed control points for PALSAR. A second order polynomial function gives a RMS error 0.27 for PALSAR.
- A Principal Component (PC) spectral sharpening algorithm was adopted to perform the data fusion in ENVI 5.0.

The second step is the automatic extraction of small lineaments. Automatic extraction requires high image resolution as in SPOT5 (band 1, 2, 3 and panchromatic at 5m×5m) to be used by the line module in PCI-Geomatica package. Field measurements and digital geological structure data digitized from Egyptian Geological Survey maps (1:250000) and other previous published maps, were compared with the extracted results from processed satellite images. Rose diagram was used to reveal the orientations of steeply dipping joints and dykes (Fig. 1 & 2). The measurements of joints and dykes were analyzed with Rockworks 16 package. Ground Penetrating Radar (GPR) survey was performed in the three locations [13] in the Nuweiba area to delineate the buried faults and verify the main trends of extracted faults from the previous techniques. GPR profiles were adopted in the two main directions represent Gulf of Aqaba and Gulf of Suez trends (Fig. 3). At each location, two to three GPR profiles were run with a total length of 440m.

Major fractures patterns were clearly noticeable in optical and microwave datasets. The major fractures were dissected with numerous dykes and veins which their altitudes were commonly controlled by prevailing major faults (Fig. 1). Satellite images and field studies show that the hard rock bodies have much more linear features than the soft terrain. All the data sources (SPOT5/SAR fused image, field studies, and GPR) in the study suggest that the major faults in the Nuweiba area were affected by Red Sea Rifting system because that the identified faults are parallel to the Gulf of Aqaba fault trend NE-SW strike and the Gulf of Suez fault trend NW-SE direction.

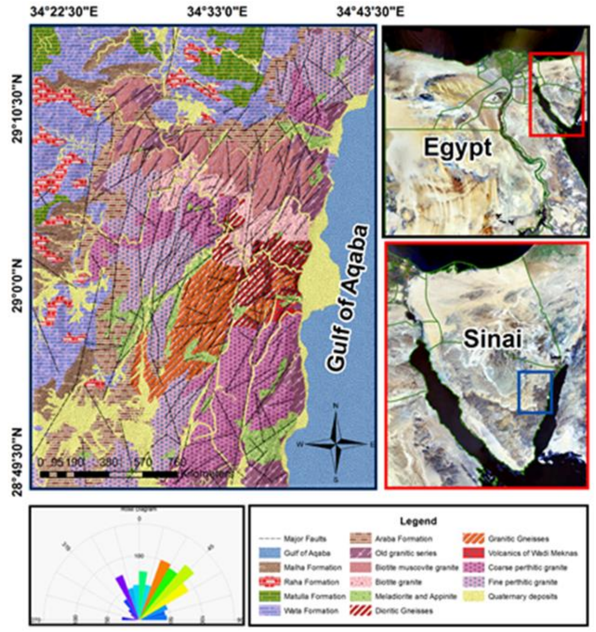

Figure 1. The location map of Nuweiba area shows different lithological units and major faults. The directions and lengths of these faults were defined using rose diagram.

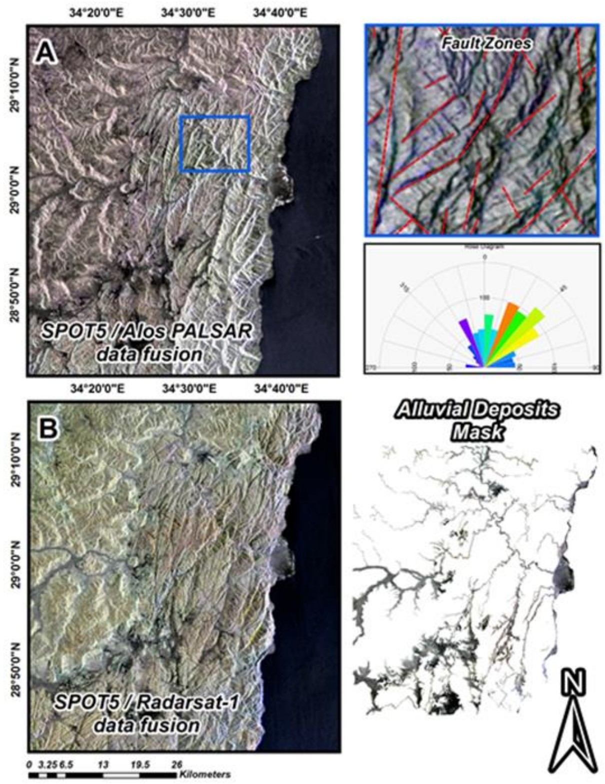

Figure 2. A- The SPOT5/ALOS PALSAR hybrid image for extracting the structural features. B- The SPOT5/Radarsat-1 hybrid image for extracting the textural characteristics of alluvial deposits (alluvial deposits mask was applied to restrict the classification to alluvial areas).

III. Thematis Layers

A. Geological Characteristics

Three important thematic layers were used to represent geological characteristics of the study area. These layers include lithological units, lineaments density and density of the lineament intersection. Using the maximum likelihood classification, we identified 16 different classes for rock units. The classes include Gulf of Aqaba, dioritic gneisses, meladiorite, granitic gneisses, old granitic series, coarse perthitic granite, fine perthitic granite, volcanics of Wadi Meknas, biotite granite, muscovite biotite granite, Raha Formation, Wata Formation, Malha Formation, Mutalla Formation, Araba Formation and Quaternary deposits (Fig. 1). Rainfall can penetrate through fissures in most of the older granitic series to reach aquifers.

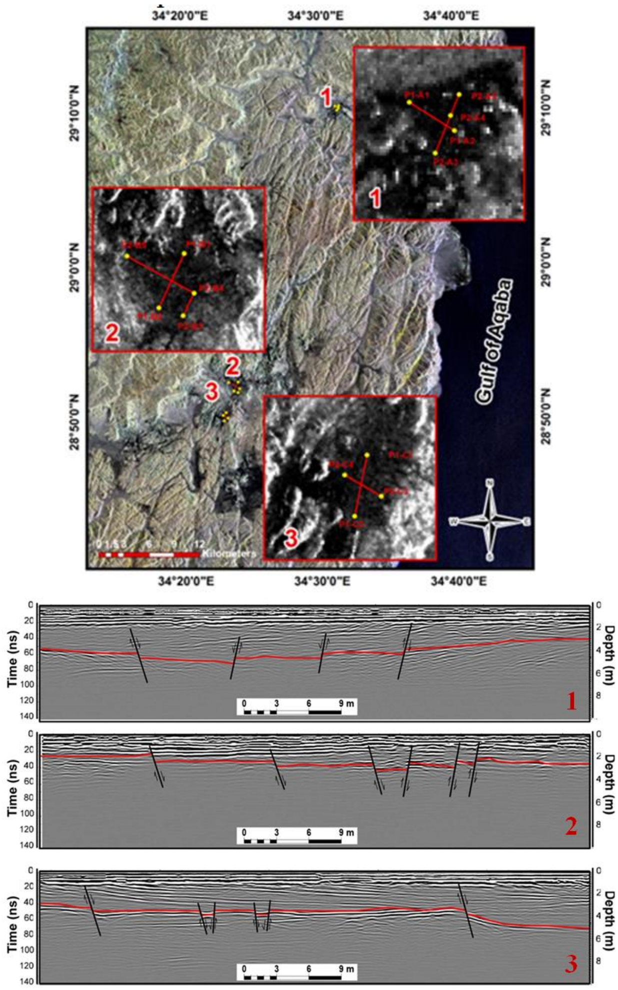

Figure 3. Surveyed sites 1, 2 and 3 where 8GPR profiles were scanned using a 270 MHz antenna showing the trends of buried faults.

The lineaments density and the density of lineament intersections were extracted using the line density analyst extension [14] of Arc View GIS. They were classified into three classes from low to high density. Further major faults, which are mega lineaments, were also identified and considered in our model. These faults showing offsets of ridges and drainage lines and were verified in the field.

B. Topographic Parameters

Shuttle Radar Topography Mission (SRTM) data was used to derive a Digital Elevation Model (DEM) at a spatial resolution of 29m DEM. The elevation and slope angle derived from the DEM are two of the keys factors to groundwater discharge. The elevation of Nuweiba area varies from 33 m and 1581 m above sea level. The slope map (0-68.6^0) with a 29-m grid cell size was classified into five classes. Most of the study area has slope in the 15° to 25° and 25° to 35° classes, while steep slopes greater than 35° are much less frequent in the area.

C. Geomorphological Parameters

The geomorphological units play a significant role in groundwater prospects. Various geomorphological units were delineated from multispectral satellite images and SRTM. High pass and edge detector convolution filters for spatial enhancement, linear contrast stretching and histogram equalization of radiometric enhancement techniques were applied on Landsat ETM+7 and SPOT5 data. Principal component analysis (PC1, PC2, and PC3) was also performed to classify the geomorphological units. The slope map prepared from SRTM DEM was used in conjunction with processed ETM+7 and SPOT5 False Color Composites (FCCs). In addition, longitudinal curvature and plan convexity were extracted from SRTM DEM. The K-means clustering algorithm was used to define natural groupings. Several band combinations were considered for the classification of landforms. The best combination results were achieved for three input parameters with standardized slope, longitudinal curvature and plan convexity and for two input parameters with standardized slope and longitudinal curvature. The classification results were grouped into seven major Landform types including peaks, ridges, scarps, terraces, plains and channels.

SRTM DEM and topographic maps at the scales of 1:50,000 were used respectively to digitize main stream channels. The digitized drainage networks were used as known streams and lake boundaries in terrain processing to guide hydrological feature extraction. The drainage density was computed as the 'total length of streams and expressed as km/km^2. The drainage density was classified with equal intervals into low (0 to 0.6 km/km^2), moderate (0.6 to 1.2 km/km^2), and high (1.2 to 1.8 km/km^2) density.

D. Textural Characteristics of Alluvial Deposits

Alluvial deposits of W. Watir were classified based on grain size distribution using multisource data fusion. Generally, Radar data were used to compute surface roughness, grain size and moisture content. In the case of flat regions with dry smooth texture of fine deposits, radar low backscatter appears dark owing to specular reflection of the radar wave away from the receiving antenna [15]. Whereas radar high backscatter indicates a rugged area with coarse deposits or rocky surfaces, and appears bright due to diffuse reflection [15]. Multisource data fusion was adopted for texture analysis using SPOT 5 (1, 2, 3 & panchromatic) and Radarsat-1, 2000 (C-band) images (Fig. 2). The process applied several techniques, including geo-referencing, geocoded and calibration of SAR dataset, speckle reduction of the SAR image, PCI data fusion and unsupervised classification.

In order to classify SPOT5/SAR fused image, the soil-adjusted-vegetation-index (SAVI) was used to perform a vegetation mask which restricts the classification to alluvial areas (Fig. 2). This step is essential to reduce the number of output classes from SPOT5/SAR image, which greatly improves their interpretability. The alluvial areas of W. Watir were derived from the SPOT5/SAR fused image using an unsupervised classification of K-means clustering algorithm considering 10 initial classes and five iterations. This classification procedure was adopted because deposits of W. Watir appeared spectrally and texturally very diverse. The deposits of W. Watir consist of a whole range of rock types and fragment sizes. The K-means clustering technique suggests the natural clusters in the fused dataset. The SPOT5/SAR classified images were filtered using a 5×5 kernel size to remove noise from the data (spurious class pixels due to radar speckle), thus, reducing the variance within the resulting clusters.

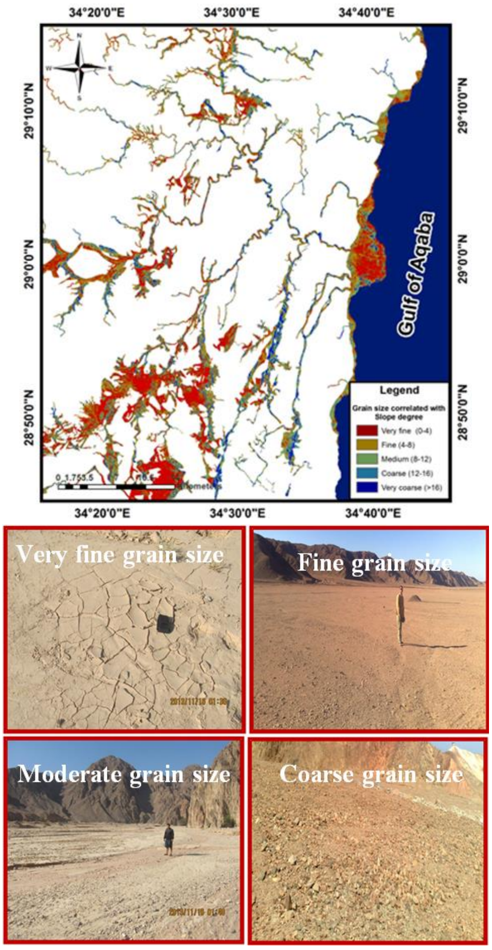

Figure 4. Unsupervised classification of the alluvial deposits using fused SPOT5/ALOS PALSAR was checked in the field. Field photographs displaying the typical grain/fragment size of each hybrid image class from very fine to coarse.

The K-means classification of the SPOT5/SAR fused image resulted in five classes. These classes were checked in the field to recognize their ground appearances (Fig. 4). These classes represent surface types in wadi deposits which indicate the surface roughness and thus the backscatter signal. According to field investigation and unsupervised classification (Fig. 4), class 5 represents the highest surface roughness and thus the strongest backscatter signal which indicate very coarse grains. Class 1 represents the smoothest surface type within the alluvial areas of W. Watir basin which indicates generally low values of backscatter signals in SAR dataset. Class 2, class 3, and class 4 represent surfaces with gradually increasing roughness or backscatter coefficient values and are situated between the smoothest class 1 and the roughest class 5 (Table I). In short, the K-mean clusters reflect the amount of backscatter (due to the SAR component) and a lesser extent to variations in hue and saturation (due to the SPOT5 component).

The output classes of the textural analysis were correlated with slope map using the Zonal Statistics as Table function in ArcGIS 10.2 (Table I). The spatial correlation between the fused image classes and slope indicates that the higher class numbers tending to occur at steeper slopes. The final output map of W. Watir deposits were used as a high weighted thematic layer in the final weighted analysis.

TABLE I. RELATIONSHIPS BETWEEN RADAR BACKSCATTER, SURFACE ROUGHNESS, AND SLOPE, AND ITS IMPLICATION IN TERMS OF GROUNDWATER-RECHARGE POTENTIAL.

Class Number	Radar σ0 values	Roughness and grain size	Slope	Groundwater recharge
Class 1	Very low backscatter	Very fine (smooth surface)	0-4	Very High
Class 2	Low backscatter	Fine	4-8	High
Class 3	Moderate backscatter	Medium	8-12	Moderate
Class 4	High backscatter	Coarse	12-16	Low
Class 5	Very high backscatter	Very coarse (Rough surface)	>16	Very Low

IV. DATA INTEGRATION

The thematic layers were integrated spatially to determine groundwater potential. Ranks of the thematic layers and weights of their classes were assigned according to their contribution to groundwater potential. The DRASTIC model, which is used to assess groundwater pollution vulnerability by the Environmental Protection Agency of United States of America [16], was modified in the current study to define the groundwater potential zones. The hydrogeological model was developed based on nine thematic layers including textural classification of alluvial deposits, slope, lineament density, geomorphology, geology, elevation, lineaments intersections, drainage density and land use. Each factor was classified to three or five classes based on their importance to groundwater occurrences. The hydrogeological model classes were ranked also according to their magnitude of contribution to groundwater entrapment. The classes were categorized from very good to very poor contribution for groundwater potential mapping (Table II). The final map consists of groundwater potential classes e.g. very good, good, moderate, poor, and very poor. The weights and ranks were adopted by the extracted factors based the experience of the first author about the study area, field investigations for the distribution of the groundwater wells and the knowledge of experts in the previous similar works on groundwater potentiality mapping [2], [17]. The ranks of each factor were modified several times to define the most favorable zones of the groundwater occurrences which match the published groundwater potential map of Sinai [18]. However, our groundwater potential map adds new locations for groundwater exploration. The Groundwater Potential Index (GWPI) was derived using equation 1 where the input the weights of input layers were multiplied by their corresponding ranks and were added.

$$\mathbf{GWPI} = \sum_{k=1}^{9} \boldsymbol{W_{ki}} \times \boldsymbol{R_k} \tag{1}$$

Based on the field investigations, most of the groundwater wells which were recorded associated with the locations of fine grain texture and gentle slope. Therefore, textural classification of alluvial deposits was assigned the highest rank and the maximum weight was assigned to very fine grain size. The slope layer was considered as the following important thematic layer (Table II). Generally, flat and gently sloping areas promote infiltration and groundwater recharge, while steeply sloping grounds encourage runoff resulting in little or no infiltration. Hence, the gentle slope was assigned the maximum weight because that the overland flow distributes over a large area and recharge would be much more in gentle sloping terrains than rugged terrains [2].

Lineament density for groundwater exploration was important because that the joints and fractures serve as conduits for movement of groundwater and have a high water-holding capacity. Hence, the high weight value for a groundwater potential area was assigned to the areas with high lineament density. Due to the importance of lineament density for the groundwater occurrence, it should be taken as fourth factor and it would be assigned 7 as rank value (Table II). Lineaments intersections are one of the important elements also in defining the groundwater favorable zone. The density of the lineaments intersections was assigned 6 as rank value where the highest density of the lineaments intersections has the highest weight.

Different land form types including plains, channel, pediments, terraces, scrapes, peaks, and ridges were checked their potential for groundwater occurrences in the field. The channels have very good groundwater potential due to valley fill deposits of unconsolidated materials providing groundwater storage. The drainage channels in the basement are controlled by geological structures. The drainage channels and the valley fill deposits can form an integrated aquifer system. Hence, the channels were assigned the maximum weight. The distribution of the groundwater wells was moderate in the plains and terraces; thus, they have moderate to good groundwater potential. Pediments also have moderate groundwater potential. Scarps and ridges have poor to very poor groundwater potential. Peaks have no groundwater potential. Therefore, scarps, ridges and peaks were assigned the lowest weight. Due to the importance of landforms types for the groundwater occurrence, it would be assigned 5 as rank value (Table II). The influence of hydraulic properties such as permeability in the lithological units causes different rates of discharge at each unit. The permeability range for different lithological units was assessed in several studies [19], [20]. The studies indicated that alluvial deposits have a high ability to infiltrate rainfall through them while Precambrian has low permeability. Therefore, alluvial deposits were given a higher weight than basement rocks. (Table II). The lithology layer was assigned 4 as rank value for the model because of its importance for groundwater occurrence.

TABLE II. RANKS (R) AND WEIGHTS (W) FOR THEMATIC LAYERS AND THEIR CLASSES IN ACCORDANCE WITH THEIR RELATIVE IMPACTS TO GROUNDWATER OCCURRENCE

Thematic layers	Classes	Groundwater potentiality	R	W
Textural Classification of Alluvial Deposits	Very fine grain size	Very good	9	9
	Fine	Good		6
	Moderate grain size	Moderate		3
	Coarse	Poor		1
	Very coarse grain size	Very poor		0
Slope	0 - 5.36	Very good	8	9
	5.36 - 14.21	Good		6
	14.21 - 23.59	Moderate		3
	23.59 - 34.59	Poor		1
	34.59 - 68.37	Very poor		0
Lineaments density	0 – 0.883	Poor	7	3
	0.883 - 1.76	Moderate		6
	1.76 -2.56	Good		9
Density of lineaments intersections	0 – 0.896	Poor	6	3
	0.869 - 1.79	Moderate		6
	1.79- 2.69	Good		9
Geomorphology	Peaks	Very poor	5	0
	Scarps and ridges	Poor		1
	Pediments	Moderate		3
	Plains and Terraces	Good		6
	Channels	Very good		9
Lithology	Quaternary deposits	Very good	4	9
	Clastic rocks	Good		6
	Carbonates rocks	Moderate		3
	Older Granite series	Poor		1
	Metamorphic and younger Granite series	Very poor		0
Elevation	0 - 3027.5	Very good	3	9
	3,027.5 - 6055.1	Good		6
	6055.1 - 9082.6	Moderate		3
	9082.6 - 12110.1	Poor		1
	12110.1 - 15137.7	Very poor		0
Drainage density	0 – 0.6	Good	2	9
	0.6 – 1.2	Moderate		6
	1.2 – 1.8	Low		3
Land use	Water bodies, build up and communities area	Very good	1	9
	Sandy desert and Sand beach	Good		6
	Drainage and roads	Moderate		3
	Stony desert	Poor		1
	Bare rock	Very poor		0

The elevation layer influences the occurrence for groundwater in the Nuweiba area. Elevated land rarely contains loose sediments within stream and the thickness of remaining sediment is often very small due to steep slope. Therefore, the occurrence of groundwater at high land should be small. On the contrary, the thickness of alluvial loose sediments on low land is likely high and along with the gentler slope, the possibility of groundwater occurrence is high. It is evident that more than 15 wells are dug at the downstream of W. Watir while about 10 wells are dug at its upstream parts. Hence, the high elevated land should take low weight for groundwater potential while the low land will get high weight for groundwater occurrence (Table II). For the model, the elevation layer was assigned 3 as a rank value.

Drainage pattern is a good indicator of hydrogeological features, because drainage pattern, texture, and density are controlled in a fundamental way by the underlying lithology [21]. The shape of the stream network reflects the likelihood of precipitation to permeate into groundwater storage. The terrain containing the greater drainage density, usually has a less permeable top soil layer which mean the denser drainage network is, the less the recharge rate is [22]. Hence, the drainage density was considered as a negative factor to permeability, which means the high density class takes a low weight while the low density area gets a high weight grade (Table II). The drainage density factor was assigned a rank of 2 in the hydrogeological model.

The land use and land cover layer consists of stony desert, sandy desert and dunes, bare rock, build up area, Bedouin communities and water bodies. Generally, The Bedouin communities reside in the Nuweiba area between the mountains around the locations of the groundwater wells. Therefore, the Bedouin Communities were assigned the highest weight while the bare rock and stony desert were assigned the lowest weight. The Land use layer was assigned a rank of 1 in the hydrogeological model.

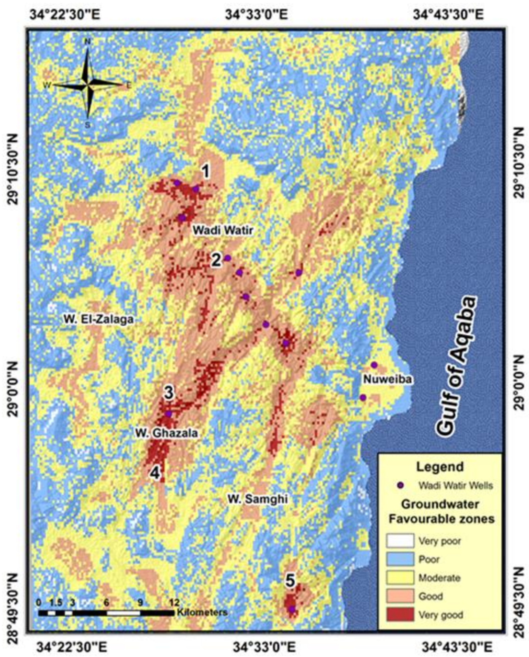

Figure 5. The groundwater potential map of Nuweiba area was checked with high spatial resolution Google Earth images.

V. Results and Validation

The final groundwater potential map consists of five major classes including very poor to very good potentiality (Fig. 5). The produced groundwater potential map suggests the promising localities for groundwater accumulations which are almost always located at areas where the surface rocks are highly permeable, which are found at the downstream of W. Watir, W. El-Zalaga, W. Ghazala, W. Samghi, W. Nekhel, and W. Sada El-Beida. The identified high groundwater potential areas are located mainly at the eastern part of Watir basin, especially in alluvial deposits and Cambrian rocks (Fig. 5). Regions of very good ranking for groundwater potential cover 5.4% of Nuweiba's total area, whereas regions characterized by very poor groundwater potential rank cover 0.9% of Nuweiba's total area. The good groundwater potential rank occupies 25.9% of the mapped area, while the poor potential rank covers about 32.5% of Nuweiba area. The moderate groundwater potential rank occupies the largest area of Nuweiba's total area representing 35.3% of the mapped area (Fig. 5).

The evaluation of the groundwater potentiality map was checked against the distribution of the groundwater wells, Bedouin communities and agriculture area in Nuweiba, which reflects the overview of groundwater potential. The groundwater potential zones match with these indicators for the sustainability of groundwater occurrences (Fig. 5). These indicators were obtained during field surveys and high spatial resolution satellite images (Google Earth). Most of the Bedouin communities and agriculture areas are located at zones of high to very high groundwater potential W. Watir's wells are located at a zone ranked good to very good. The final potential map has a high degree of confidence especially it adds new locations for groundwater exploration. It indicated that the main stream of W. Watir and W.

Ghazala represent an excellent area for groundwater exploration. In addition to, the downstream of W. Samghi and W. Sada El-Beida represent very good areas for groundwater exploration.

The upstream of W. Watir should be considered also as the promising area for groundwater exploration. These zones represent gentle slope, low to moderate drainage density and widely spread sedimentary rocks and alluvial deposits help recharge an aquifer. Wells at the upstream area are located in moderately elevated to low elevation zones where they tap fractured basement aquifers. The distribution of granitic rocks with low fractured, high drainage density and steep slope, especially at downstream of Wadi Watir, cease the recharge of aquifers and increase the runoff and overflow during rainy seasons.

VI. Conclusion

The Nuweiba area needs a management system for groundwater recharge. Several thematic layers were prepared in the current study to define the favorable zone of groundwater occurrences. These layers include lithology, lineaments, faults, landforms, elevation and slopes. These layers were prepared from different data sources include SPOT5, Radarsat-1, ALOS PALSAR, SRTM, and GPR. These data were processed using different remote sensing and GIS techniques. Multisource data fusion is most suitable technique to extract the structural elements and textural characteristics of the alluvial deposits. Finally, all thematic layers were assigned different ranks and their classes assigned different weights according to their importance for groundwater occurrences. The weights and ranks of the different thematic maps were derived based on authors experiences, field survey and previous studies. The final groundwater potential map suggest new promising areas for groundwater accumulations which are found at the downstream of W. Watir, W. El-Zalaga, W. Ghazala, W. Samghi, W. Nekhel, and W. Sada El-Beida.

Acknowledgment

The authors wish to thank the Ministry of Higher Education and Scientific Research in Egypt for the financial support of this research.

References

[1] P. Sander, M. Chesley, and T. Minor, "Groundwater assessment using remote sensing and GIS in a rural groundwater project in Ghana: Lessons learned," *Hydrogeology Journal*, vol. 4, no. 3, pp. 78-93, 1996.

[2] S. Solomon and F. Quiel, "Groundwater study using remote sensing and geographic information systems (GIS) in the central highlands of Eritrea," *Hydrogeology Journal*, vol. 14, no. 6, pp. 1029-1041, 2006.

[3] A. Chowdhury, M. K. Jha, and V. M. Chowdary, "Delineation of groundwater recharge zones and identification of artificial recharge sites in West Medinipur district, West Bengal, using RS, GIS and MCDM techniques," *Environmental Earth Science*, vol. 59, no. 6, pp. 1209-1222, 2010.

[4] M. Muralidhar, K. R. K. Raju, K. S. V. P. Raju, and J. R. Prasad, "Remote sensing applications for the evaluation of water resources in rainfed area, Warangal district, Andhra Pradesh," *The Indian Mineralogists*, vol. 34, no. 2, pp. 33-40, 2000.

[5] P. K. Srivastava and A. K. Bhattacharya, "Groundwater assessment through an integrated approach using remote sensing, GIS and resistivity techniques: A case study from a hard rock terrain," *International Journal of Remote Sensing*, vol. 2, no. 20, pp. 4599-4620, 2006.

[6] J. Krishnamurthy, A. Mani, V. Jayaraman, and M. Manivel, "Groundwater resources development in hard rock terrain-an approach using remote sensing and GIS techniques," *International Journal of Applied Earth Observation and Geoinformation*, vol. 2, no. 3, pp. 204-215, 2000.

[7] N. S. Magesh, N. Chandrasekar, and J. P. Soundranayagam, "Delineation of groundwater potential zones in Theni district, Tamil Nadu, using remote sensing, GIS and MIF techniques," *Geoscience Frontiers*, vol. 3, no. 2, pp. 189-196, 2012.

[8] A. Gaber, M. Koch, and F. El-Baz, "Textural and compositional characterization of wadi Feiran deposits, Sinai Peninsula, Egypt, using Radarsat-1, PALSAR, SRTM and ETM+ data," *Remote Sensing*, vol. 2, no. 1, pp. 52-75, 2009.

[9] A. Gaber, M. Koch, M. H. Griesh, and M. Sato, "SAR remote sensing of buried faults: Implications for groundwater exploration in the Western Desert of Egypt," *Sensing and Imaging: An International Journal*, vol. 12, no. 3, pp. 133-151, 2011.

[10] EGSMA, Egyptian Geological Survey and Mining Authority, Geologic map of Sinai, Arab Republic of Egypt, Sheet no. 1, Scale 1: 250.000, 1994.

[11] R. G. Congalton, "A review of assessing the accuracy of classifications of remotely sensed data," *Remote Sensing of Environment*, vol. 37, no. 1, pp. 35-46, 1991.

[12] R. Said, *The Geology of Egypt*; New York: Elsevier, 1962, pp. 337.

[13] M. F. Kaiser, "GIS data integration for SRTM-Landsat ETM+-Radarsat-1 images to delineate subsurface paleolakes, wadi watir area, Egypt," in *Proc. International Geo-Science and Remote Sensing Symposium*, Jul. 2013, pp. 3594-3597.

[14] A. K. Saraf, "IRS-1C-LISS-III and PAN data fusion: An approach to improve remote sensing based mapping techniques," *International Journal of Remote Sensing*, vol. 20, no. 10, pp. 1929-1934, 1999.

[15] J. R. Jensen, "Active and passive microwave, and LIDAR remote sensing," *Remote Sensing of the Environment: An Earth Resource Perspective*, NJ: Prentice-Hall, 2000, ch. 9, pp. 285-332.

[16] L. Aller, T. Bennett, J. Lehr, and R. J. Petty, "DRASTIC: A standard system for evaluating groundwater pollution potential using hydrogeologic settings," EPA/600/2-85/018, R.S. Kerr Environmental Research Laboratory, U.S. Environmental Protection Agency, Ada, Oklahoma, 1985.

[17] G. I. Obiefuna and A. Sheriff. "Assessment of shallow ground water quality of Pindiga Gombe area, Yola Area, NE, Nigeria for irrigation and domestic purposes," *Res. J. Environ. Earth Sci.*, vol. 3, no. 2, pp. 131-141, 2011.

[18] H. Elwa and A. El Qaddah, "Groundwater potentiality mapping in the Sinai Peninsula, Egypt, using remote sensing and GIS-watershed-based modeling," *Hydrogeology Journal*, vol. 19, no. 3, pp. 613-628, 2011.

[19] A. El Naqa, N. Hammouri, K. Ibrahim, and M. El-Taj, "Integrated approach for groundwater exploration in wadi araba using remote sensing and GIS," *Jordan Journal of Civil Engineering*, vol. 3, no. 3, pp. 229-243, 2009.

[20] T. M. Baharuddin, D. Tjahjanto, A. R. Othman, A. A. Ab. Latiff, K. Masiri, and W. C. Wong, "Application of geographic information system (GIS) in demarcation groundwater potential zones," in *Proc. National Conference – Water for Sustainable Development Towards a Developed Nation by 2020, Malaysia*, Jul. 2006.

[21] E. Sener, A. Davraz, and M. Ozcelik, "An integration of GIS and remote sensing in groundwater investigations: A case study in Burdur, Turkey," *Hydrogeology Journal*, vol. 13, pp. 826-834, 2005.

[22] A. Edet, S. Okereke, C. Teme, and O. Esu, "Application of remote sensing data to groundwater exploration: A case study of the Cross River State, southeastern Nigeria," *Hydrogeology Journal*, vol. 6, no. 3, pp. 394-404, 1998.

Sara M. Abuzied received the B.S. degree in Geology from Suez Canal University in 2005 and M.S. degree in Geochemistry from Suez Canal University in 2011. She has enrolled for the Ph.D. degree in Environmental Geology since 2012 according to Twinning Degree Programs including study at Center for Spatial Analysis, University of Oklahoma, USA and Geology Department, Suez Canal University, Egypt.

From Jan. 2006 to Apr. 2011, she was Demonstrator in Geology Department. Since May 2011, she has been Assistant Lecturer in Geology Department. She is currently scientific researcher in Center for Spatial Analysis, University of Oklahoma, USA.

Her research interests include Digital Image Processing, Geospatial Statistical Analysis, Geoinformatics, Environmental Impact Assessment and Environmental Sustainability.

May Yaun received the B.S. degree in Geography, National Taiwan University, 1987 and M.A. degree in Geography, State University of New York at Buffalo, 1992 and Ph.D. Geography, State University of New York at Buffalo, 1994.

She is currently Ashbel Smith Professor of Geospatial Information Sciences in University of Texas at Dallas, USA.

Samia K. Ibrahim received the B.S. degree in Geology from Suez Canal University in 1976 and M.S. degree in Geochemistry from Suez Canal University in 1989 and Ph.D degree in Geochemistry from Suez Canal University in 1995.

She is currently Professor Emeritus of Igneous and Metamorphic Rocks in Suez Canal University, Egypt.

Mona F. Kaiser received the B.S. degree in Geology from Suez Canal University in 1988 and M.S. degree in Sedimentology from Suez Canal University in 1996 and Ph.D degree in Remote Sensing and GIS from University of Reading, UK in 2004.

She is currently Associate Professor of Remote Sensing and GIS in Suez Canal University, Egypt.

Tarek A. Seleem received the B.S. degree in Geology from Suez Canal University in 1995 and M.S. degree in Structural Geology from Suez Canal University in 2001 and Ph.D degree in Structural Geology from Suez Canal University in 2005. He is currently Assistant Professor of Structural Geology in Suez Canal University, Egypt.